

Research Paper

Mediation of the JNC/ILC2 pathway in DBP-exacerbated allergic asthma: A molecular toxicological study on neuroimmune positive feedback mechanism

Xiaomin Xie^a, Yan Li^{a,e}, Biao Yan^a, Qi Peng^a, Runming Yao^b, Qihong Deng^c, Jinqian Li^d, Yang Wu^a, Shaohui Chen^a, Xu Yang^a, Ping Ma^{a,*}

^a Key Laboratory of Environmental Related Diseases and One Health, Xianning Medical College, Hubei University of Science and Technology, Xianning 437100, China

^b Joint International Research Laboratory of Green Buildings and Built Environments (Ministry of Education), Chongqing University, Chongqing 400045, China

^c School of Public Health, Zhengzhou University, Zhengzhou 450001, China

^d Brain Science and Advanced Technology Institute, School of Medicine, Wuhan University of Science and Technology, Wuhan 430065, China

^e Department of Pharmacy, Ezhou Central Hospital, Ezhou 436000, China

HIGHLIGHTS

- DBP can exacerbate allergic asthma via a neuroimmune regulatory mechanism.
- DBP can induce activation of TRPV1 and JNC neurons, and then make CGRP releases.
- Th2-dominant inflammation happens following ILC2 activation by CGRP.
- IgE is the key molecular for triggering type I hypersensitivity and JNC reactivation.

GRAPHICAL ABSTRACT



ARTICLE INFO

Editor: Dr. S Nan

Keywords:

Dibutyl phthalate (DBP)

Allergic asthma

Neuroimmune positive feedback regulation

Jugular nodose ganglion complex (JNC)

ABSTRACT

Background: Dibutyl phthalate (DBP), a commonly used plasticizer, has been found to be strongly linked to a consistently high prevalence of allergic diseases, particularly allergic asthma. Previous animal experiments have demonstrated that exposure to DBP can worsen asthma by triggering the production of calcitonin gene-related peptide (CGRP), a neuropeptide in the lung tissue. However, the precise neuroimmune mechanism and pathophysiology of DBP-exacerbated allergic asthma with the assistance of CGRP remain unclear.

Abbreviations: DBP, dibutyl phthalate; OVA, ovalbumin; T-IgE, total immunoglobulin E; OVA-IgE, ovalbumin specific immunoglobulin E; OVA-IgG1, ovalbumin specific immunoglobulin G1; AHR, airway hyperresponsiveness; Ri, inspiratory resistance; Re, expiratory resistance; Cldyn, lung compliance; MCH, acetylcholine; H&E, hematoxylin and eosin staining; MT, Masson trichrome staining; PAS, periodic acid-schiff staining; JNC, jugular nodose ganglion complex; FcεRI, IgE high-affinity receptor; TRPV1, transient receptor potential vanilloid subtype 1; [Ca²⁺]_i, intracellular calcium ions concentration; CGRP, calcitonin gene-related peptide; ILC2, group 2 innate lymphoid cell; CLR, calcitonin receptor-like receptor; Olcegepant, CLR specific antagonist; MAPK, mitogen-activated protein kinase; GATA3, GATA binding protein 3; PGATA3, phosphorylated GATA binding protein 3; ST2, growth stimulation expression gene 2 protein; CD45, cluster of differentiation 45; CD90.2, cluster of differentiation 90.2.

* Correspondence to: Hubei University of Science and Technology, No. 88 Xianning Avenue, Xianning 437100, China.

E-mail addresses: mping68@126.com, mapping@hbstu.edu.cn (P. Ma).

<https://doi.org/10.1016/j.jhazmat.2023.133360>

Received 15 October 2023; Received in revised form 18 December 2023; Accepted 21 December 2023

Available online 23 December 2023

0304-3894/© 2023 Elsevier B.V. All rights reserved.

Group 2 innate lymphoid cells (ILC2)
 Calcitonin gene-related peptide (CGRP)
 GATA binding protein 3 (GATA3)

Objective: The present study was to investigate the potential pathophysiological mechanism in DBP-exacerbated asthma from the perspective of neural-immune interactions.

Methods and results: C57BL/6 mice were orally exposed to different concentrations (0.4, 4, 40 mg/kg) of DBP for 28 days. They were then sensitized with OVA and nebulized with OVA for 7 consecutive excitations. To investigate whether DBP exacerbates allergic asthma in OVA induced mice, we analyzed airway hyperresponsiveness and lung histopathology. To investigate the activation of JNC and TRPV1 neurons and the release of CGRP by JNC cells, we measured the levels of TRPV1 channels, calcium inward flow, and downstream neuropeptide CGRP. Results showed that TRPV1 expression, inward calcium flux, and CGRP levels were significantly elevated in the lung tissues of the 40DBP + OVA group, suggesting the release of CGRP by JNC cells. To counteract the detrimental effects of DBP mediated by CGRP, we employed olcegepant (also known as BIBN-4096), a CGRP receptor specific antagonist. Results revealed that 40DBP + OVA + olcegepant led to notable decreases in TRPV1, calcium inward flow, and CGRP expression in lung tissues compare with 40DBP + OVA, further supporting the efficacy of olcegepant. Additionally, we also conducted ILC2 flow sorting and observed that neuropeptide CGRP-activated ILC2 cells have a crucial role as key effector cells in DBP-induced neuroimmune positive feedback regulation. Finally, we examined the protein expression of CGRP, GATA3 and P-GATA3, and found that significant upregulations of CGRP and P-GATA3 in the 40DBP + OVA group, suggest that GATA3 acted as a key regulator of CGRP-activated ILC2.

Conclusion: The aforementioned studies indicate that exposure to DBP can exacerbate allergic asthma, leading to airway inflammation. This exacerbation occurs through the activation of TRPV1 in JNC, resulting in the release of CGRP. The excessive release of CGRP further promotes the release of Th2 cytokines by inducing the activation of ILC2 through GATA phosphorylation. Consequently, this process contributes to the development of airway inflammation and allergic asthma. The increased production of Th2 cytokines also triggers the production of IgE, which interacts with FcεR1 on JNC neurons, thereby mediating neuro-immune positive feedback regulation.

1. Introduction

Asthma is a significant global public health issue [50] and is among the most expensive chronic diseases [55]. Allergic asthma, which affects over half of all asthma patients [41], is the most common type. Research on the mechanism of allergic asthma has demonstrated that immunoglobulin E (IgE) binds to the high-affinity receptor for IgE (FcεR1) on mast cells, leading to the release of inflammatory factors. This process plays a crucial role in the development of allergic asthma [12,31]. The conventional pathogenesis theory of allergic asthma involves the type I hypersensitivity mediated by Th2 cells. The excessive production of Th2-related cytokines contributes to the progression of allergic asthma [20]. The impact of environmental factors on allergic asthma has grown in popularity [27–29]. Multiple studies have established a close association between environmental pollutants and the pathogenic factors of asthma [15,47,53].

Phthalates (PAEs), the most widely produced and consumed plasticizer in the world, are extensively used in various applications such as interior construction, food packaging, medical equipment, and personal care products. PAEs are combined with plastic substrates through non-covalent bonds, making them easily released into the environment (including air, water, soil, etc.), and they are considered ubiquitous environmental pollutants [18]. Among the different types of PAEs, DBP is particularly prevalent. As a low molecular weight phthalate, DBP is commonly found in both indoor and outdoor environments and can enter the human body through inhalation, ingestion, and skin contact [25]. The European Food Safety Authority (EFSA) sets an acceptable daily intake of 10 µg/kg d⁻¹ [39] DBP. Numerous studies have indicated a strong association between DBP and the development of allergic asthma [1]. Epidemiological and toxicological studies have provided evidence for the “environmental adjuvant” effect of DBP-induced allergic asthma [47], but the underlying mechanisms and pathophysiological processes remain unclear, leading to a lack of targeted prevention and treatment strategies.

The previous research conducted at the animal level demonstrated that exposure to DBP can worsen asthma-like symptoms induced by allergens through the regulation of the neuropeptide calcitonin gene-related peptide (CGRP) in lung tissue (Zhou et al., 2022). Several studies have discovered that the increase in IgE levels can enhance the reactivity of FcεR1 on the jugular nodose ganglion complex (JNC) neurons. The combination of IgE and FcεR1 can activate the transient

receptor potential vanilloid subtype 1 (TRPV1), leading to the release of the neuropeptide CGRP and its involvement in the expansion of the inflammatory cascade response in lung tissue [2,3,6]. The induced elevation of IgE levels is a characteristic feature of the “environmental adjuvant” effect of DBP. Based on this, we hypothesize that DBP, acting as an “environmental adjuvant”, may cause an upregulation of neuropeptide CGRP expression in lung tissue by activating JNC neurons and TRPV1.

Group 2 innate lymphocytes (ILC2) are a type of innate immune cells that play a crucial role in connecting innate and acquired immunity in lung tissue. These cells are known to produce IL-4, IL-5 and IL-13, and their involvement in the development of allergic asthma has been well-established [34,49]. The neuropeptide CGRP has been found to be expressed by JNC cells in lung tissue and has been shown to activate ILC2, contributing to the progression of allergic diseases [21,46,5]. Based on this, we hypothesize that neuropeptide-activated ILC2 may be the key effector cells in the positive feedback regulation of neuro-immune response induced by DBP. CGRP, a neuropeptide that plays a crucial role in the pathogenesis of asthma, acts as a bridge between nerves and immune regulation, amplifying allergic asthma responses [44]. Previous studies have demonstrated that the binding of calcitonin receptor-like receptor (CLR) on the surface of ILC2 can activate MAPK pathways, leading to GATA phosphorylation, proliferation, and activation of ILC2, ultimately resulting in the release of large quantities of Th2 cytokines. The transcription factor GATA3 has been identified as the master regulator in this process [24,51]. Therefore, we propose that GATA3 plays a key role in regulating CGRP-activated ILC2.

In the present study, we investigated the mechanism by which DBP acts as an environmental adjuvant in exacerbating allergic asthma. Our focus was on understanding the neuroimmune interactions involved in this process. Specifically, we examined the impact on the activation of JNC neurons and TRPV1, the production of the neuropeptide CGRP, and the subsequent activation of ILC2. Additionally, we identified the significant role of GATA3 in CGRP-regulated ILC2 activation. Our research should contribute to the field by providing practical applications and scientific evidence for the prevention and control of health risks and hazards associated with phthalate pollutants.

2. Materials and methods

2.1. Animals

SPF-grade C57BL/6 J male mice, aged between 6–8 weeks, were purchased from Liaoning Changsheng Biotechnology Co., Ltd. (batch number: SCXK (Liao) 20200001). After purchase, the mice were adaptively fed for one week and provided with a commercial diet and filtered water *ad libitum*. Throughout the experiment, the mice were maintained at a room temperature of $(24 \pm 2)^\circ\text{C}$, relative humidity of $(50 \pm 5)\%$, and a light/dark cycle of 12 h/12 h. Humane care was provided to the mice following the 3 R principles used in experimental animals. All procedures were authorized by the Research Management Office of Hubei University of Science and Technology, and a certificate of approval (ID: HBUST-IACUC-2021–010) is available upon request.

2.2. Reagents and instruments

DBP ($\geq 99\%$, CAS: 84–74–2), OVA, and methacholine (MCH) were purchased from Sigma-Aldrich. Tween-80 (CAS: 9005–65–6) was purchased from Amresco (Solon, OH, USA). T-IgE (total-IgE), OVA-IgE, OVA-IgG1, Interleukin 4 (IL-4), Interleukin 5 (IL-5), Interleukin 13 (IL-13), Interleukin 25 (IL-25), and Interleukin 33 (IL-33) ELISA kits were purchased from Shanghai Enzyme Biotechnology Co., Ltd. (Shanghai, China). The Power waveXS microplate reader and ELx800 fluorescent microplate reader were purchased from Bio-Tek Instruments Co., Ltd. of the United States. The HH-42 three-purpose electric heating constant temperature water tank was purchased from Beijing Changyuan Experimental Instrument Factory, and the 5424 R low-temperature refrigerated centrifuge was purchased from Eppendorf, Germany. The DP73 microscope was purchased from Japan Olympus Company.

2.3. Experimental protocol

Referring to the data published by the European Chemicals Bureau [10], this study set up a low-dose exposure group (0.4 mg/kg) based on a concentration close to the detected concentration of DBP in drinking water (0.47 mg/L), and a medium-dose was set at 4 mg/kg based on a concentration close to the detected concentration of DBP in surface water (4.8 mg/L) from Europe, the United States and Asia. Naturally, a high dose of 40 mg/kg was set to observe the dose-effect relationship. The mice were randomly divided into 7 groups, each consisting of 30 mice. These groups included: (1) saline group, (2) 0.4 mg/kg DBP group, (3) 4 mg/kg DBP group, (4) 40 mg/kg DBP group, (5) OVA group, (6) 40 mg/kg DBP + OVA group, and (7) 40 mg/kg DBP + OVA + olcegepant (in short “+olcegepant”) group. After one week of adaptive feeding, mice requiring exposure to DBP were gavaged from day 1 to day 28. Mice requiring OVA sensitization were intraperitoneally injected with an OVA sensitization solution on days 9, 12, 15, 18, and 21. From days 29 to 35 of the experimental cycle, 1% OVA was nebulized for one week, with each session lasting 30 min. The +olcegepant group received intraperitoneal injections of 1 mg/kg/day olcegepant (CLR specific antagonist) from days 1 to 36. The experimental scheme was presented

Table 1
Grouping and experimental treatments.

Group ID	Group names	Treatments for different groups				
		Gavage 0.4 DBP	Gavage 4.0 DBP	Gavage 40 DBP	OVA oral exposure	Olcegepant I.P. injection
Group 1	Saline	–	–	–	–	–
Group 2	0.4DBP	+	–	–	–	–
Group 3	4.0DBP	–	+	–	–	–
Group 4	40DBP	–	–	+	–	–
Group 5	OVA	–	–	–	+	–
Group 6	40DBP+OVA	–	–	+	+	–
Group 7	40DBP+OVA +Olcegepant	–	–	+	+	+

in Table 1 and Fig. 1.

A total of 210 mice were used in this study, with 30 mice in each group. Ten mice in each group were used for ventilation and alveolar lavage fluid. The other twelve mice were used for cardiac blood collection, the right lungs were immobilized in paraformaldehyde for section preparation, and the left lungs were used for lung tissue homogenate preparation. The remaining eight mice were divided into two batches, and tested for western blot and ILC2 flow sorting, respectively.

2.4. Serum and tissue preparation

Following a 36-day period, mice received an intraperitoneal injection of 100 mg/kg pentobarbital sodium. The chest wall was cleaned using alcohol-soaked cotton balls, after which an incision was made to expose the heart. Approximately 0.8–1.0 mL of blood was carefully withdrawn from the heart using a 1 mL medical syringe and transferred into a 1.5 mL centrifuge tube. The blood was then subjected to centrifugation at 25°C for 10 min and 3000 rpm. After discarding the supernatant, it was preserved at -80°C for future utilization. The serum derived from the blood was employed for the detection of T-IgE, OVA-IgE, and OVA-IgG1. Subsequently, both lungs were excised after blood collection from the heart. The right lung was directly fixed in paraformaldehyde, while the left lung was rinsed with 10% cold PBS (pH = 7.4) and dried using absorbent paper. The left lung was then homogenized with 10% PBS solution and maintained at 4°C at 10,000 rpm for 10 min. The resulting supernatant was stored at -80°C . This lung supernatant was utilized for the determination of IL-4, IL-5, IL-13, IL-25 and IL-33.

2.5. Pathology and immunohistochemistry of lung sections

We excised and relocated the right lung, and then proceeded to fix the lungs using a 4% paraformaldehyde solution. To prepare the tissue for analysis, a sequential immersion in alcohols of varying grades and xylenes was employed. Finally, the tissue was embedded in paraffin following a traditional approach. After 24 h, sections of $4\ \mu\text{m}$ thickness were deparaffinized and mounted on glass slides. Hematoxylin and eosin (H&E), Masson’s trichrome staining (MT), periodic acid-schiff staining (PAS), and immunohistochemical detection were then performed. Immunohistochemical analysis was conducted after antigen retrieval and inactivation of endogenous enzymes, following the method described by Yan et al. [52].

2.6. Lung function test

Mice were anesthetized with 100 mg/kg sodium pentobarbital [30]. After achieving deep anesthesia, the neck skin was incised to expose the trachea. Subsequently, a tube was inserted into the trachea and connected to a ventilator (Bestlab, AniRes 2005, version 2.0, China). The ventilator settings were adjusted to maintain a respiratory/inspiratory ratio of 1.5:1 and a respiratory rate of 90 breaths per minute. Throughout the operation of the AniRes2005 software, the jugular vein was injected with $50\ \mu\text{L}$ of MCH every 5 min. The injected

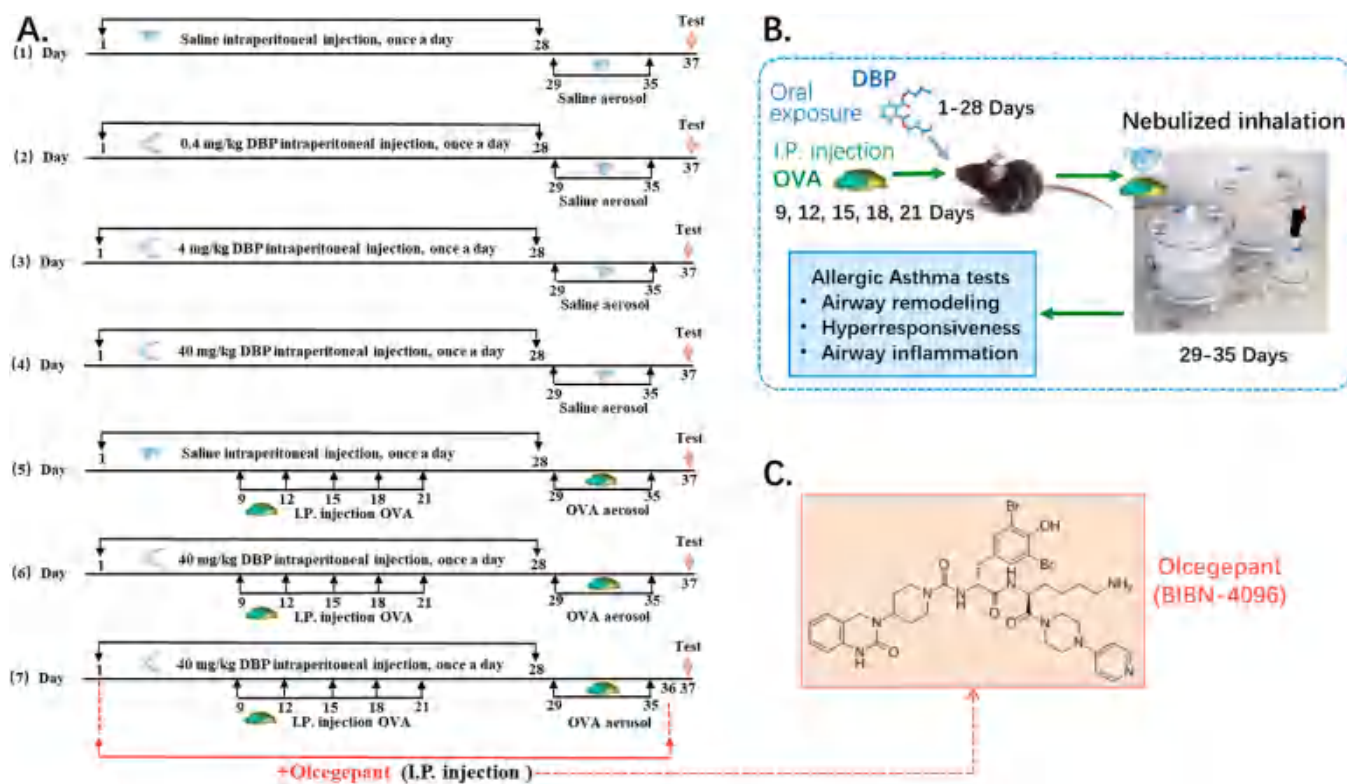


Fig. 1. Experimental protocol. (A) Grouping and experimental schedule; (B) OVA sensitization and challenge of the mice; (C) Chemical structure of olcegepant.

concentrations included 0.025, 0.05, 0.1, and 0.2 mg/kg, respectively. The AniRes2005 software continuously recorded real-time values for inspiratory resistance (Ri), expiratory resistance (Re), and lung dynamic compliance (Cldyn). The R area was defined as the enclosed region between the peak Ri or Re and the baseline within 300 s following injection. Meanwhile, lung compliance was measured using the lowest recorded value of Cldyn.

2.7. Immunoglobulin and inflammatory factor measurements

ELISA kits were utilized to quantify the concentrations of T-IgE, OVA-IgE, and OVA-IgG1 in serum, as well as the concentrations of IL-4, IL-5, IL-13, IL-25, and IL-33 in lung tissue. The experimental procedures were conducted in accordance with the instructions provided in the kit.

2.8. Detection of JNC neuron activation (calcium influx)

The fixation of each lung tissue section involved embedding, sectioning, and subsequent sequential washing with xylene, anhydrous ethanol, 85% alcohol, and 75% alcohol distilled water. To facilitate antigen recovery, the sections were placed within repair cassettes that contained EDTA antigen recovery buffer (with a pH of 8.0) and subjected to microwave-assisted antigen retrieval. A heating process was carried out on the slides, where they were heated at medium temperature for a duration of 8 min, followed by an 8-minute rest period, and then heated again at medium-low temperature for 7 min. Subsequently, the slides were placed at 4 °C and shaken three times for 5 min each on a decolorizing shaker. A circle was drawn around the tissue with a pen, and the autofluorescent bursting agent was added to the circle for 5 min, followed by a 10-minute rinse with tap water. The serum was then blocked using the serum for 30 min, and fura-2 AM (a calcium fluorescent probe, 2 mM) was added and incubated overnight at 4 °C. Next, the secondary antibody was added and incubated for 50 min, followed by the addition of DAPI staining solution, which was incubated for 10 min. After conducting a comprehensive washing and drying process, the

sections were tightly sealed using an anti-fluorescence burst mounting medium. Subsequently, an observation of the sections was carried out utilizing a Nikon microscope (Eclipse 80i, Tokyo, Japan). Our indicator test referred to [6].

2.9. Flow cytometric analysis of ILC2 cells

The mice were anesthetized using intraperitoneal injection of pentobarbital. The skin was disinfected with 75% alcohol, and the thoracic cavity was opened under aseptic conditions to remove the lung tissue. The lung tissue was then placed on a sterile 200 mesh nylon mesh in a 60 mm cell culture dish. It was gently ground using a 2.5 mL syringe plunger and washed with 5 mL of 1640 medium to obtain a final lung cell suspension. The lung cell suspension was transferred to a 15 mL centrifuge tube and centrifuged at 1500 rpm for 5 min at room temperature to remove the supernatant. Next, 3 mL of red blood cell lysate was added to lyse the cells at room temperature for 4 min, followed by resuspending the cells. The cells were then washed with 10 mL of sterile PBS, centrifuged again at 1500 rpm for 5 min at room temperature to remove the supernatant, and resuspended in 1 mL of 1640 complete medium. For ILC2 sorting, lung cells were stained with CD45 (eBioscience, San Diego, CA, USA), CD90.2 (eBioscience, San Diego, CA, USA), and ST2 (BioLegend, San Diego, CA, USA). Lin-CD45 + ST2 + CD90.2 + cells were sorted into ILC2 using FACS Aria (BD Biosciences, NJ, USA). Our indicator test referred to [40].

2.10. Swiss Jim staining of alveolar lavage fluid

The right major bronchus was ligated using forceps while the mice were under anesthesia. Subsequently, PBS was perfused through the right ventricle and gently aspirated over the left lung for lavage. For each animal, three 0.5 mL of PBS were prepared. After the third lavage with PBS, the fluid recovered from the lungs was collected as bronchoalveolar lavage fluid (BALF). Cytoцентрифуг slides were stained with May-Giemsa to determine cell differentials. The supernatants of

BALF were promptly stored at -80°C until analysis.

2.11. Western blot detection

Protein expression levels of CGRP, GATA3, P-GATA3, and ST2 were analyzed using Western blot. An equal amount of protein extract from each sample was separated and transferred to a PVDF film using 12.5% SDS-PAGE (EpiZyme, Shanghai, China). Each membrane was then incubated overnight at 4°C with antibodies against CGRP, GATA3, P-GATA3, and ST2 (Affinity, Jiangsu, China). Subsequently, the membrane was incubated with the appropriate HRP Goat Anti-Mouse IgG (H+L) secondary antibody (ABclonal, Wuhan, China) at room temperature for 2 h. Image J software (Bio-Rad Laboratories, Hercules, CA, USA) was used for imaging.

2.12. Statistical analysis

We utilized GraphPad Prism 9.0 software (GraphPad Software, San Diego, USA) for statistical analysis and graph generation. The data are presented as mean \pm sem. The normal distribution was determined using the D'Agostino Pearson omnibus test. To compare multiple groups, we performed a one-way ANOVA followed by Bonferroni tests. For the analysis of airway hyperresponsiveness (AHR) results, we employed two-way ANOVA and multiple comparison tests. Flow cytometry data were analyzed by CyExpert2.3 software (Beckman Coulter, United States). A P value of < 0.05 was considered statistically significant.

3. Results

3.1. Lung function changes

The changes in lung function of mice primarily involved alterations

in inspiratory resistance (Ri), expiratory resistance (Re), and lung compliance (Cldyn) (Fig. 2). The Ri and Re values increased with the concentration of methacholine, while the Cldyn value decreased. The DBP group showed slight changes in Ri, Re, and Cldyn compared to the saline group. The OVA group and DBP+OVA group exhibited significant changes, with Ri and Re significantly increasing and Cldyn significantly decreasing. In comparison to the DBP+OVA group, the +olcegepant group showed significant decreases in Ri and Re, while Cldyn significantly increased.

3.2. Lung histopathological changes

H&E staining results revealed significant inflammatory infiltration, airway deformation, increased airway wall folds, and airway wall thickening in the OVA group and DBP+OVA group, particularly in the DBP+OVA group, when compared to the saline group. However, after intervention with olcegepant, there was an alleviation of airway deformation, reduction in inflammatory infiltration, and thinning of the airway walls (Fig. 3A). Masson staining, which highlights collagen fibers in blue, showed evident collagen fibrosis near the airway in the OVA group and DBP+OVA group, especially in the DBP+OVA group, compared to the saline group. Nevertheless, after intervention with olcegepant, there was a significant reduction in collagen fibers near the airway (Fig. 3B). PAS staining, which makes goblet cells appear pale pink, was used to assess the proliferation of goblet cells in the bronchial mucosa and understand the severity of asthma. The results demonstrated noticeable hyperplasia of goblet cells near the airway in the OVA group and DBP+OVA group, particularly in the DBP+OVA group, when compared to the saline group. However, after intervention with olcegepant, there was a significant reduction in goblet cell hyperplasia near the airway (Fig. 3C).

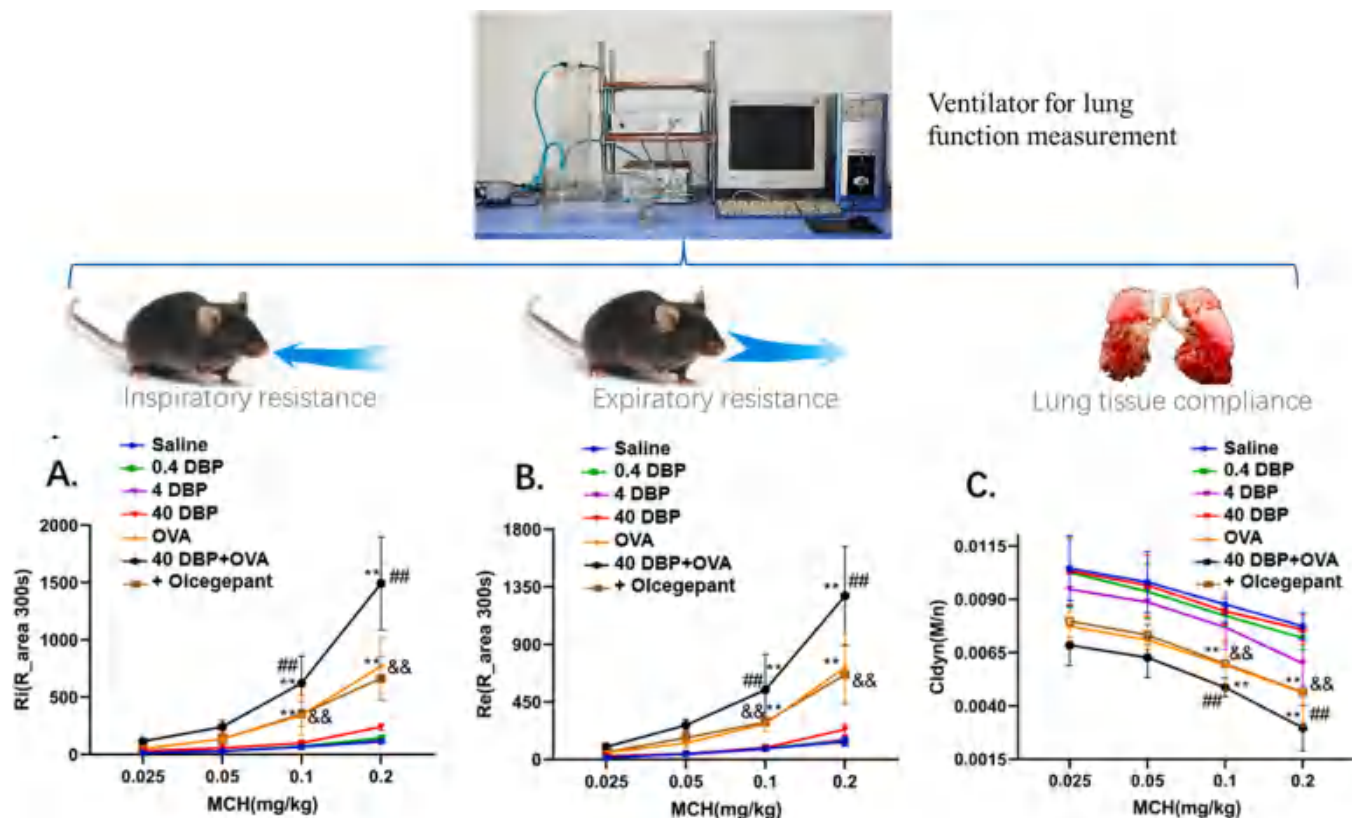


Fig. 2. AHR measurements. (A), (B), and (C) represent Ri, Re, and Cldyn values of the different treatment groups, respectively. (**: $P < 0.01$, compared with the saline group; ##: $P < 0.01$, compared with the OVA group; &&: $P < 0.01$, compared with the 40 DBP+OVA group).

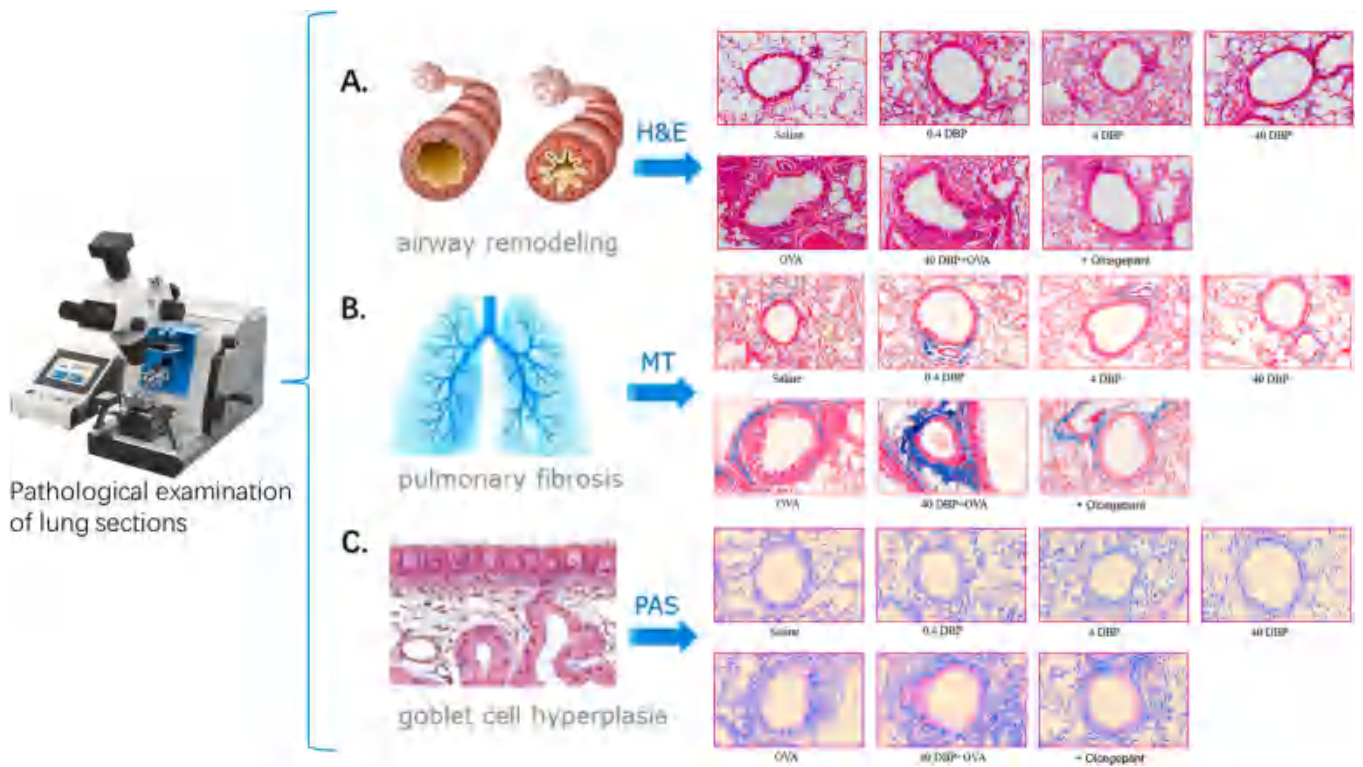


Fig. 3. Lung histopathology. (A) Hematoxylin and eosin staining (H&E) (40 ×); (B) Masson trichrome staining (MT) (40 ×); (C) Periodic acid-schiff staining (PAS) (40 ×).

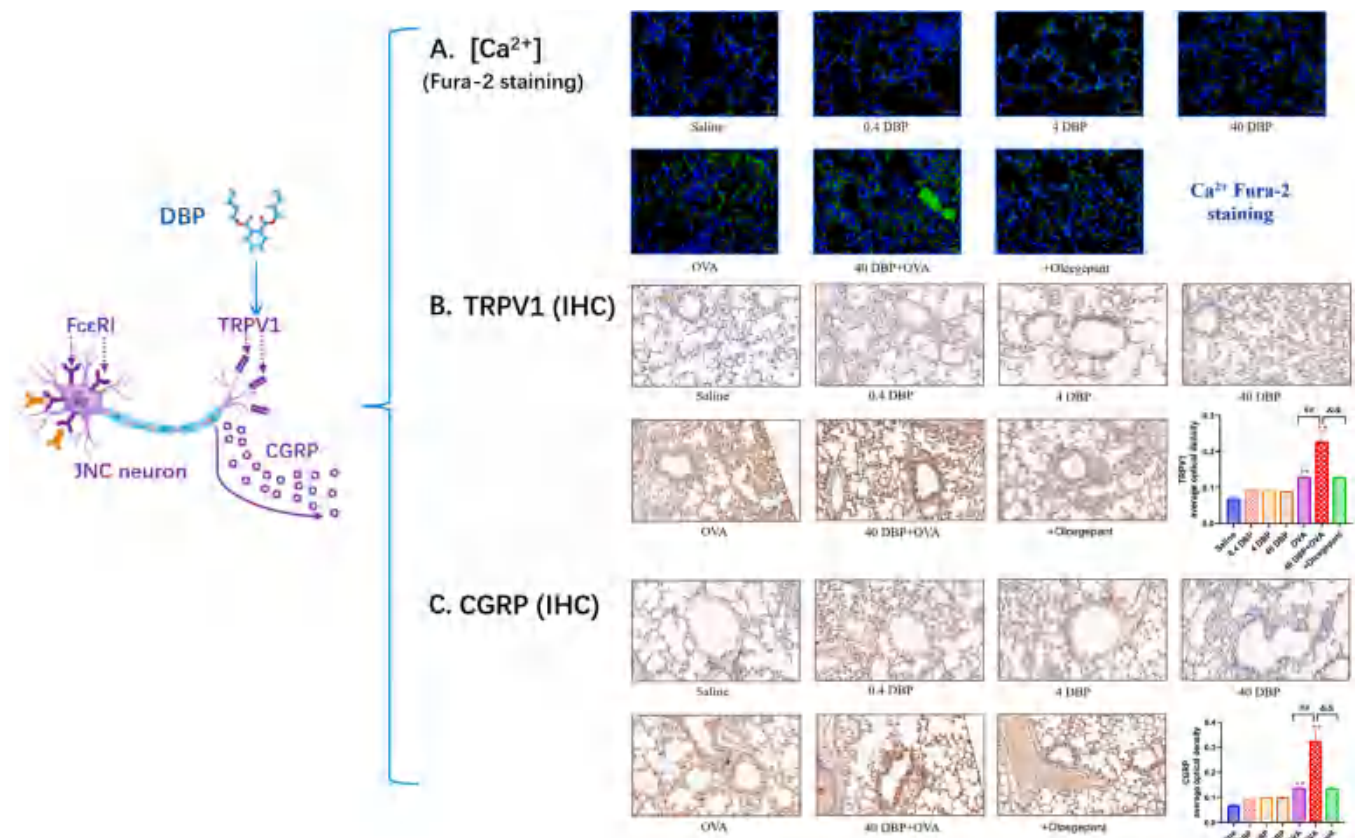


Fig. 4. JNC neuron activation: [Ca²⁺] and related IHC biomarkers. (A) Fura-2 staining (40 ×); (B) TRPV1 immunohistochemistry (40 ×); (C) CGRP immunohistochemistry (40 ×). (**: $P < 0.01$, compare with saline group; #: $P < 0.01$, comparison between OVA group and 40DBP+OVA group; &&: $P < 0.01$, comparison between 40 DBP+OVA group and 40DBP+OVA+olcegepant group).

3.3. JNC neuron activation: $[Ca^{2+}]$ and related IHC biomarkers

Fura-2, a specific fluorescent indicator of intracellular calcium ion concentration ($[Ca^{2+}]$), was used to detect the inflow of calcium in pulmonary nerve cells and the activation of JNC neurons. The results demonstrated that compared to the saline group, the fluorescence (green) was enhanced in the OVA group and the DBP+OVA group, indicating a significant increase in calcium inflow, particularly in the DBP+OVA group. Following intervention with olcegepant, the fluorescence was attenuated, leading to a significant reduction in cell calcium inflow and inhibition of JNC neuron activation (Fig. 4A).

TRPV1 and CGRP play important roles in the JNC/ILC2 pathway, similar to cell calcium inflow $[Ca^{2+}]$. TRPV1 is a chemoreceptor in neuronal membranes and a cation channel. When stimulated by DBP, it activates and opens up the ion channel, resulting in cell calcium inflow and the release of the neuropeptide CGRP. TRPV1 and CGRP not only participate in signaling, but also serve as biomarkers for detecting JNC neuronal activation. The application of IHC assay revealed enhanced IHC color in the OVA and DBP+OVA groups compared to the saline group, particularly in the DBP+OVA group. However, after intervention with olcegepant, the color was weakened, indicating the inhibition of

JNC neuronal activation (Figs. 4B and 4C).

3.4. ILC2 immune cells activation related biomarkers

Group 2 innate lymphoid cells (ILC2) are a type of innate immune cell that act as a significant source of Th2 cytokines IL-4, IL-5, IL-13. Biomarkers associated with ILC2 can be divided into two groups. The first group consists of pathway signaling components, including CGRP, CLR, IL-25, IL-33, ST2 (IL-33R), GATA3, PGATA3, IL-4, IL-5, IL-13, and eosinophils (EOS). These components play a role in the signaling cascade from upstream to downstream. TRPV1 activation causes the release of pro-inflammatory mediators such as CGRP, which mediates neurogenic inflammation, and IL-33 release upregulates ST2 receptor expression in ILC2s. The levels of CGRP, ST2 and IL-33 were slightly increased in the DBP group compared to the saline group, and the levels of CGRP, ST2 and IL-33 were significantly increased in the OVA and DBP+OVA groups. Those proteins levels were significantly increased in the DBP+OVA group compared to the OVA group, and that levels were significantly decreased and significantly different in the DBP+OVA+olcegepant group compared to the DBP+OVA group (Figs. 5A and 5C). No significant change in EOS levels in the DBP group

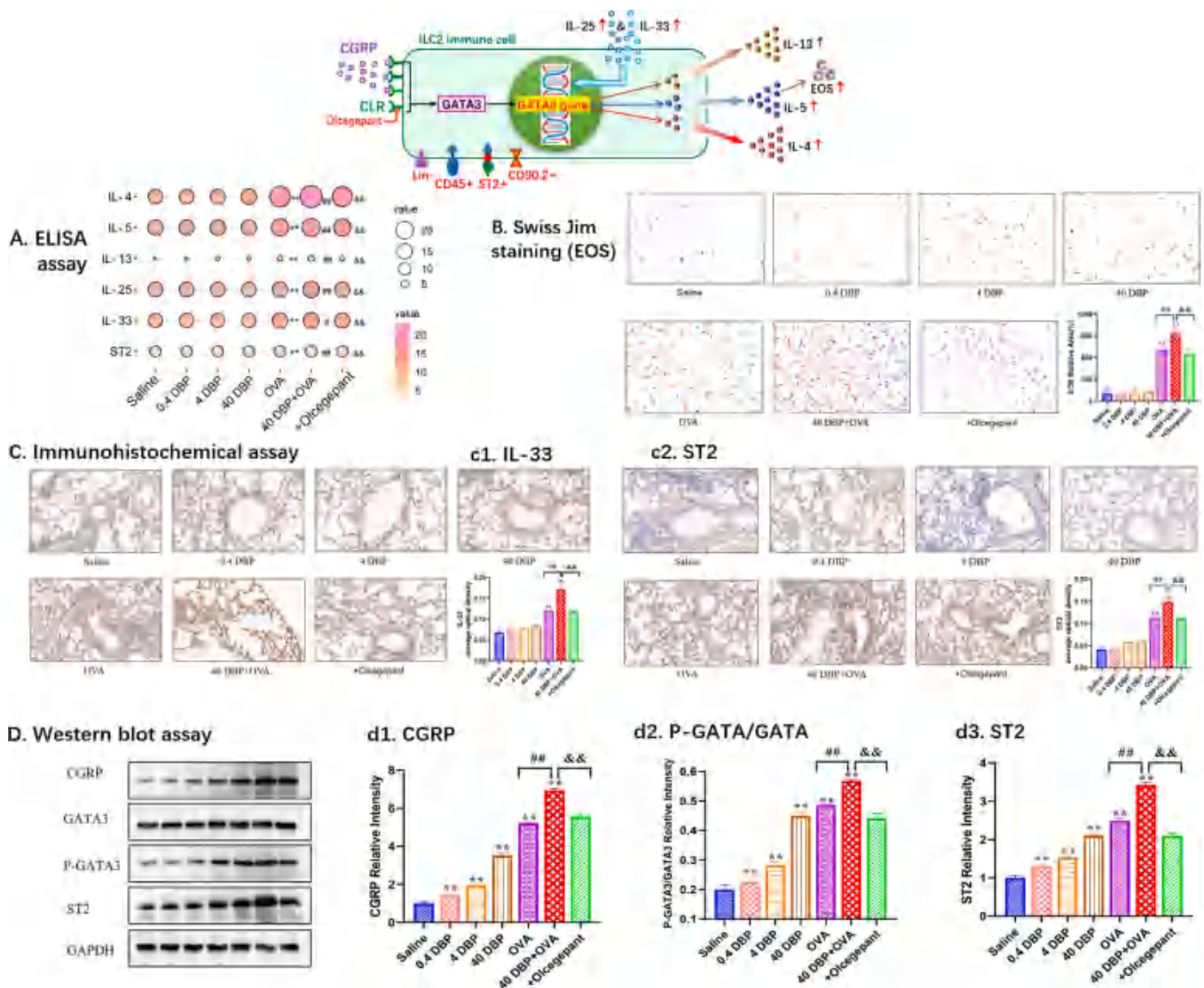


Fig. 5. Results of the ILC2 activation related biomarkers. (A) ELISA for 6 proteins; (B) Swiss Jim staining for EOS; (C) IHC for IL-33 and ST2; (D) Western blot for CGRP, GATA, PGATA, GATA, and ST2 (**: $P < 0.01$, compare with saline group; ##: $P < 0.01$, comparison between OVA group and 40DBP+OVA group; &&: $P < 0.01$, comparison between 40 DBP+OVA group and 40DBP+OVA+olcegepant group).

compared to the saline group, and significant increases in the OVA and DBP+OVA groups; however, the intervention with olcegepant resulted in a significant decrease in EOS levels (Fig. 5B). GATA-3 induces Th2 cytokine gene expression, P-GATA3 /GATA3 can be used to indicate the phosphorylation level of GATA-3. The results showed that the

expression of P-GATA3 /GATA3, CGRP, and ST2 was significantly up-regulated in different concentrations of DBP group, OVA group, and DBP+OVA group compared to the saline group. The expression of P-GATA3 /GATA3, CGRP, and ST2 was significantly up-regulated in the DBP+OVA group compared to the OVA group, while the expression of P-

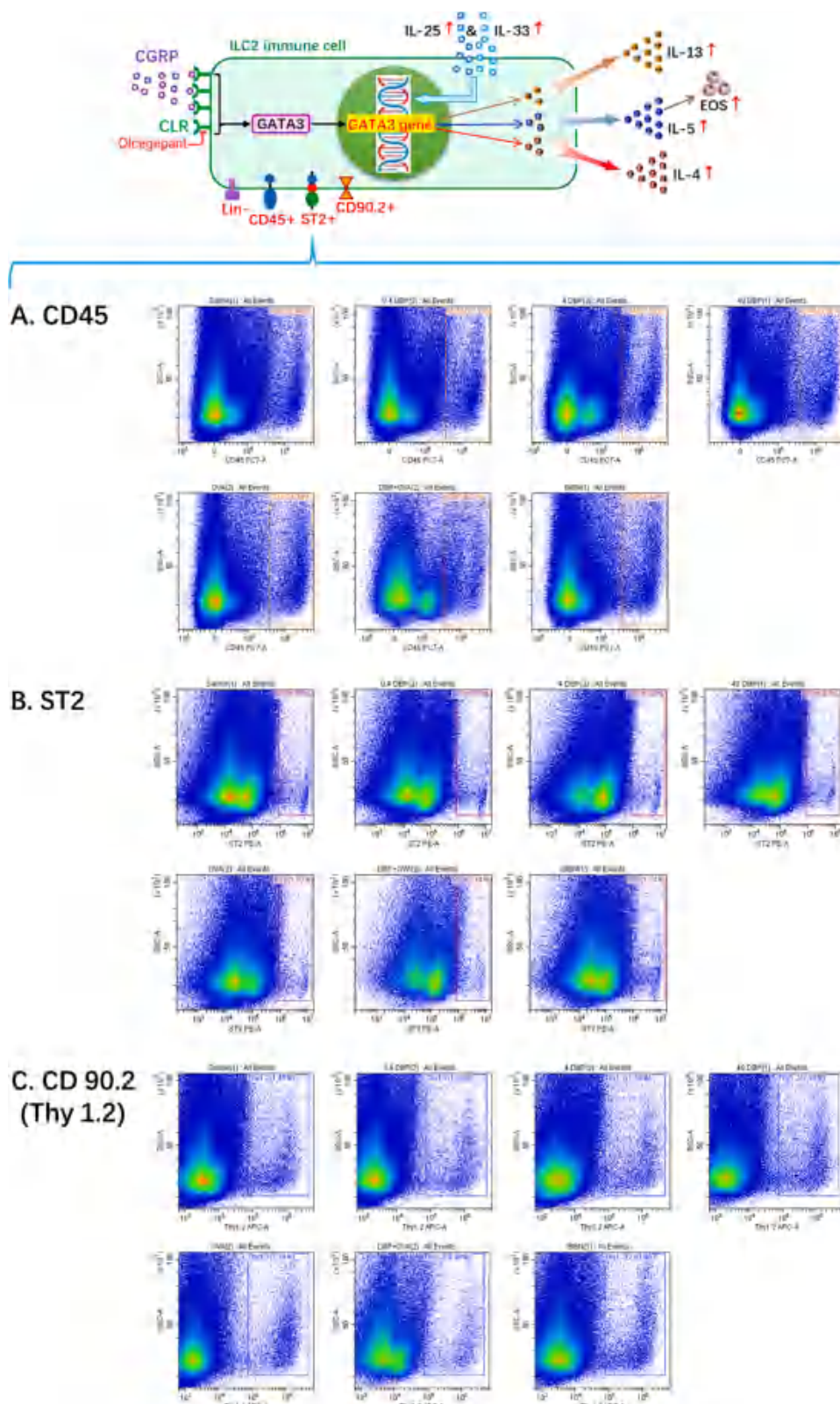


Fig. 6. Flow analysis results of ILC2s cells in lung tissues after DBP exposure. (Cell sorting for (A) CD45, (B) ST2, and (C) CD90.2).

GATA3 /GATA3, CGRP, and ST2 was significantly down-regulated in the olcegepant group compared to the DBP+OVA group (Fig. 5D).

The second group includes markers used to identify the differentiation and maturation of ILC2, such as CD45, ST2 and CD90.2 (also known as Thy1.2). Using Lin- CD45 + ST2 + Thy1.2 + as a mouse ILC2 cell marker, flow cytometry was applied to detect OVA-sensitized asthma model after DBP exposure. The results showed that Lin-CD45 + ST2 + Thy1.2 + levels were significantly increased in the DBP+OVA group in a concentration-dependent relationship compared to the saline group group. After the intervention with CGRP receptor antagonist olcegepant, Lin- CD45 + ST2 + Thy1.2 + levels in the 40 mg/kg DBP+OVA+ olcegepant group decreased significantly. These data supported that ILC2 may be key effector cells in DBP-induced neuro-immune positive feedback regulation (Fig. 6, Table 2).

3.5. Type I hypersensitivity related biomarkers

Immunologically, allergic asthma is classified as a type I hypersensitivity disease. For humans, the main biomarkers are T-IgE and antigen-specific IgE. In mice, such as C57BL/6, antigen-specific IgG1 is also involved in the development of type I hypersensitivity. The results of serum immunoglobulin detection in each group of mice are shown in Fig. 7. The levels of T-IgE, OVA-IgG1, and OVA-IgE antibodies in the DBP+OVA group (40 mg/kg) were significantly higher than those in the OVA group ($P < 0.01$). After intervention with the antagonist olcegepant, the levels of these biomarkers were significantly reduced compared to the DBP+OVA group ($P < 0.01$). Furthermore, the immunoglobulin levels in all three groups were significantly higher compared to the saline group ($P < 0.01$).

4. Discussion

Our scientific hypothesis: In this study, we utilized the OVA-induced allergic asthma C57BL/6 mouse model to investigate the potential involvement of neuro-immunity in the exacerbation of allergic asthma in mice due to DBP exposure. Through a comprehensive review of relevant literatures and analysis of our experimental findings, we propose the following scientific hypothesis (Fig. 8). This neuro-immune positive feedback mechanism consists of the following steps: (1) DBP induced activation of JNC neuron: After exposure, DBP enters the lung tissue of the organism and acts on the chemoreceptor TRPV1 of JNC neurons. The activation of TRPV1 leads to calcium inward flow and activation of the JNC neurons, resulting in the release of the neuropeptide CGRP. (2) CGRP induced activation of ILC2 immune cell: The released CGRP acts at CLR on the membrane of ILC2, activating the GATA3 transcription factor and corresponding genes. As a result, ILC2 synthesizes and releases IL-4, IL-5, and IL-13. (3) Enhancement of type I hypersensitivity induced by excess increased IL-4: Increased levels of IL-4 can intensify the type I hypersensitivity response, leading to the production of excess IgE and IgG1, and worsening the severity of allergic asthma. (4) Re-activation of JNC caused by increased IgE: Excess IgE can also act on FcεRI receptors on the membrane of JNC neurons, triggering JNC reactivation and forming neuroimmune positive feedback.

Table 2

The levels of Lin-CD45 +ST2 +CD90.2 + in different groups.

Group ID	Group names	Levels of ILC2 markers (%)		
		CD45	ST2	CD90.2
Group 1	Saline	2.56	0.55	1.40
Group 2	0.4DBP	2.70	0.63	1.20
Group 3	4.0DBP	3.10	0.59	1.58
Group 4	40DBP	3.36	0.67	2.10
Group 5	OVA	4.78	1.02	2.34
Group 6	40DBP+OVA	8.81	2.14	3.39
Group 7	40DBP+OVA+olcegepant	4.43	1.24	2.61

Evidence of DBP exacerbating allergic asthma: Allergic asthma is a chronic respiratory disease characterized by airway hyper-responsiveness (AHR) and allergic airway inflammation ([14,23]). In this study, we observed severe AHR in mice. The results (Fig. 2) showed a significant increase in Ri and Re in the DBP+OVA group compared to the saline group and OVA group, while Cldyn was significantly decreased. Additionally, histopathological examination revealed severe airway inflammation with inflammatory cell infiltration, airway remodeling (Fig. 3A), pulmonary fibrosis (Fig. 3B), and goblet cell hyperplasia (Fig. 3C) in the lung tissue of the mice.

DBP induced activation of JNC neuron: The jugular-nodal ganglion complex (JNC) is a component of the vagus nerve that plays a role in the sensory and motor functions of the heart and lungs [42]. Recent studies have discovered a small population of JNC neurons that innervate the airways and lungs [17]. Transient receptor potential channel protein subtype V1 (TRPV1), also known as the capsaicin receptor, is a non-selective cation channel found in the nerve terminals of mammalian JNC nociceptor neurons [35]. It plays a role in the perception of thermal and certain chemicals [36]. Activation of nociceptor neurons leads to the opening of TRPV1 ion channels, which allows extracellular Ca^{2+} to enter. This influx of Ca^{2+} acts as a second messenger and contributes to the release of neuropeptides and other immunomodulators, such as CGRP [4,45]. DBP, as an environmental pollutant, can cause the opening of TRPV1 ion channels, leading to JNC activation and subsequent release of CGRP. This release of CGRP acts on immune cells, initiating a neuro-immune response that ultimately exacerbates allergic asthma [6, 11]. Our findings were consistent with those of the references mentioned above. Compared to the saline group group, both the OVA group and the DBP+OVA group showed a significant increase in intracellular calcium concentration [Ca^{2+}] (Fig. 4A) and enhanced expression of TRPV1 (Fig. 4B) and CGRP (Fig. 4C), indicating the activation of JNC neurons. However, the DBP+OVA group exhibited a more pronounced increase in [Ca^{2+}] and expression of TRPV1 and CGRP (Figs. 4A, 4B and 4C), suggesting that DBP had the ability to further enhance the degree of JNC activation.

CGRP induced activation of ILC2 immune cell: Group 2 innate lymphocytes (ILC2) are innate immune cells that play a crucial role in connecting innate and acquired immunity in lung tissue [34,49]. Activated ILC2 cells exhibit various surface antigenic profiles, primarily characterized by lineage- (i.e. Lin-), CD45 +, ST2 +, CD90.2 + [16]. ILC2 is a significant contributor to allergic asthma [34]. When activated, ILC2 cells strongly induce airway hyperresponsiveness (AHR) [37], playing a critical role in the initiation and progression of asthma [7,38]. Activated ILC2 cells produce and release numerous Th2 cytokines, including IL-4, IL-5, and IL-13. They are essential components for the initiation and transmission of inflammatory and allergic responses and promote the development of Th2 dominant inflammation in the lungs [33,54,9]. Eosinophils are key effector cells that induce airway inflammation and airway hyperresponsiveness in allergic asthma [43]. The primary activators of ILC2 include IL-25 and IL-33, which are mainly derived from epithelial and endothelial cells in the lungs [8,56].

Recent studies have shown that IL-25 and IL-33 are not the only activators of ILC2. Calcitonin gene-related peptide (CGRP) also plays a significant role in this process [6]; Wallrapp et al., 2019). CGRP is a 37-amino acid neuropeptide that belongs to the calcitonin peptide family and is found in both the peripheral and central nervous systems [26,48]. It acts as a crucial link between nerves and immune regulation by binding to the receptor CLR (calcitonin receptor-like receptor) on the surface of ILC2, thereby activating ILC2 and contributing to allergic disease processes [5,21]. Olcegepant is an effective and selective antagonist of CLR, and its use is to determine whether the JNC/ILC2 pathway is involved. GATA3 is a transcription factor, when phosphorylated GATA3 is able to enter the nucleus and initiate the expression of relevant genes. P-GATA3 plays a crucial role during the sustained expression of Th2 cytokines by all ILC2s. It is also an important component for the maintenance of ILC2 differentiation and maturation,

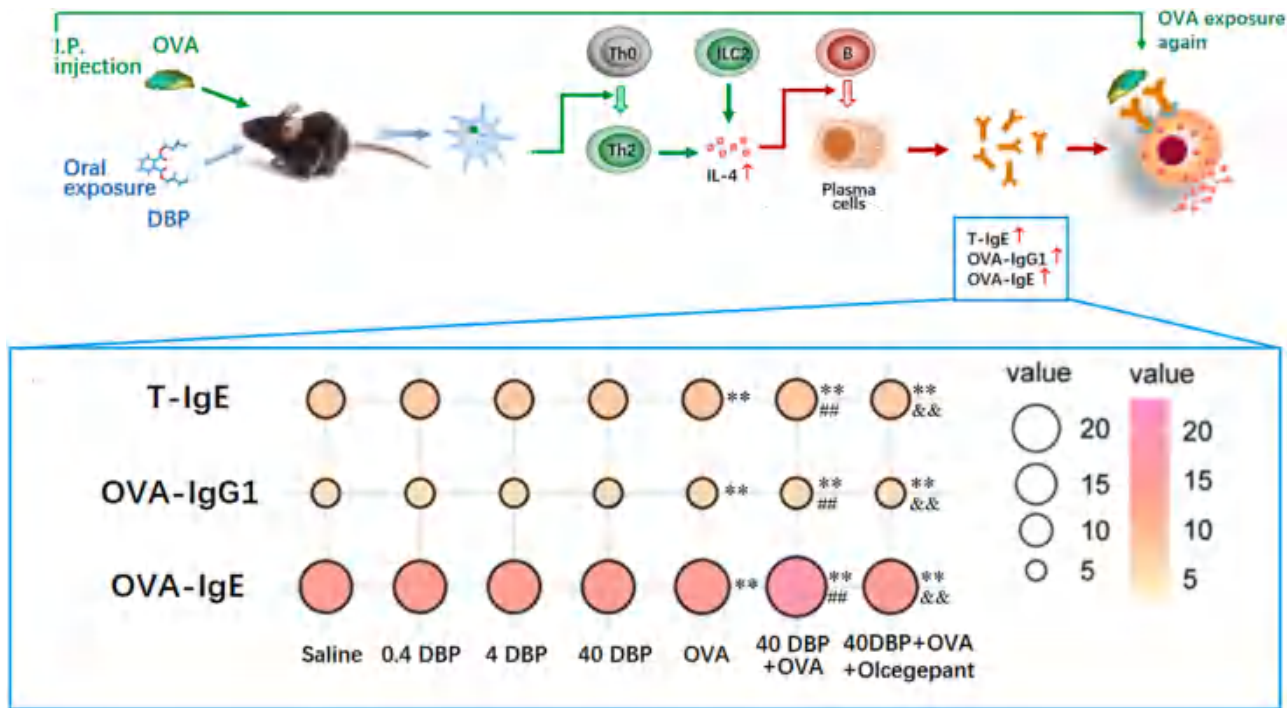


Fig. 7. Type I hypersensitivity related biomarkers. (A) Total immunoglobulin E (T-IgE); (B) Ovalbumin specific immunoglobulin G1 (OVA-IgG1); (C) Ovalbumin specific immunoglobulin E (OVA-IgE). (**: $P < 0.01$, any group compare with saline group; #: $P < 0.01$, comparison between OVA group and 40DBP +OVA group; &&: $P < 0.01$, comparison between 40 DBP+OVA group and 40DBP+OVA+olcegant group).

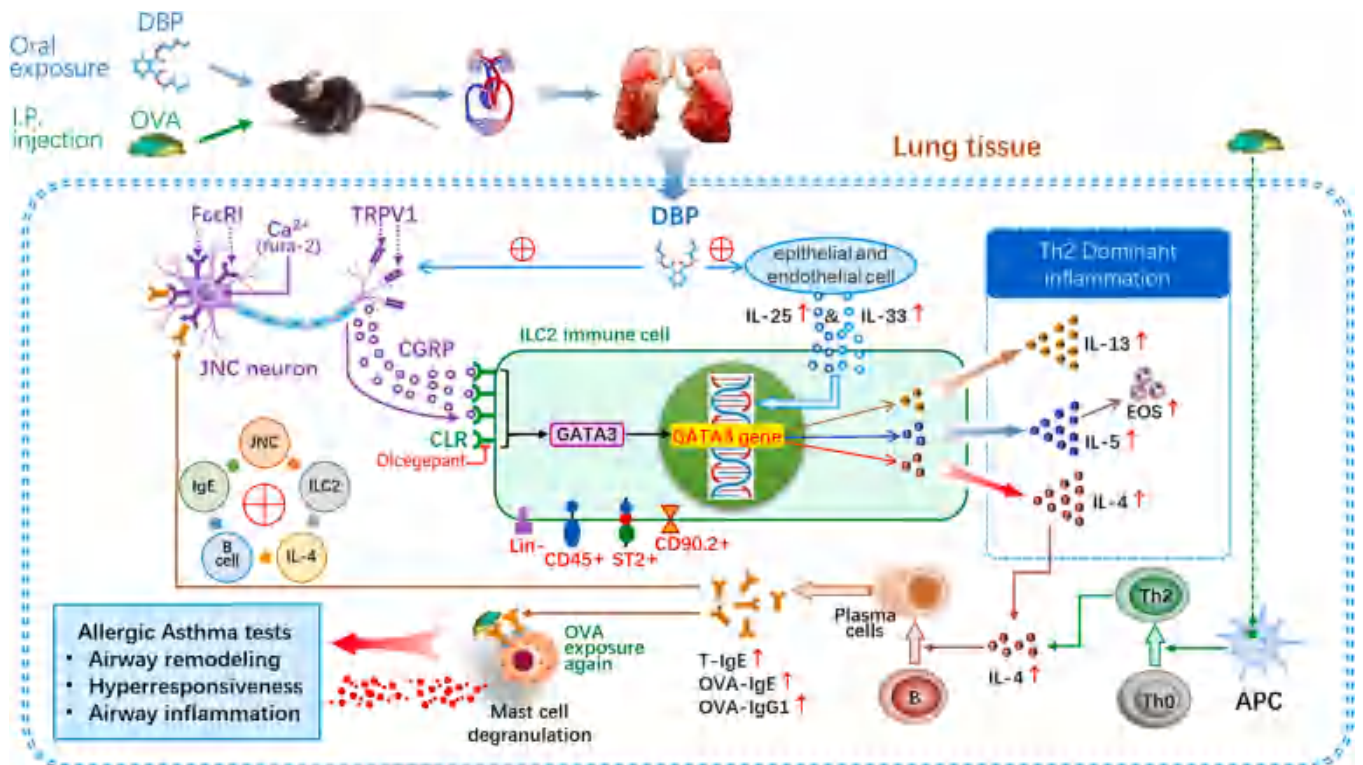


Fig. 8. Our scientific hypothesis: A potential mechanism on neuroimmune positive feedback during the DBP-exacerbating allergic asthma.

which are essential for determining ILC2 activation [13].

Our study found that various types of indices related to ILC2 showed the same trend. These included: activating factors of ILC2 such as CGRP, IL-25, and IL-33; transcription factors for activating ILC2 gene like P-GATA3/GATA3; surface antigens (cell surface markers) of ILC2 such as

CD45, ST2, and CD90.2; Th2 cytokines secreted by ILC2 like IL-4, IL-5, and IL-13; as well as IL-5-induced eosinophils. The results of the study demonstrated a significant elevation in all ILC2-related indices in the OVA and DBP+OVA groups compared to the saline group (Fig. 5, Fig. 6, and Table 2), indicating activation of ILC2 immune cells. Furthermore,

the increase in all ILC2-related indices was more pronounced in the DBP+OVA group (Fig. 5, Fig. 6, and Table 2), suggesting that DBP enhances the activation of ILC2 immune cells. When the CGRP antagonist olcegepant was administered (DBP+OVA +olcegepant group), all ILC2-associated indices were reduced compared to the DBP+OVA group. These findings support our proposed scientific hypothesis. Interestingly, the activators of ILC2, i.e. IL-25 and IL-33, which appear unrelated to the JNC/ILC2 pathway, also showed a decrease in concentration levels after intervention with the CGRP antagonist olcegepant. The biological mechanism behind this observation warrants further exploration.

Enhancement of type I hypersensitivity induced by excess increased IL-4: Allergic asthma is a chronic airway inflammation caused by allergens that can be enhanced by immune adjuvants. Immunologically, it is classified as a type I hypersensitivity reaction [19]. Type I hypersensitivity is an immune response triggered by antigen-specific IgE [22]. In rodents, such as mice, IgG1 also plays a role in mediating the type I hypersensitivity response [32]. Therefore, T-IgE, antigen-specific IgE (e.g., OVA-IgE), and antigen-specific IgG1 (e.g., OVA-IgG1) serve as important biomarkers for assessing the type I hypersensitivity response and are used as specificity indicators in asthmatic mice [20]. It is well known that in type I hypersensitivity, IgE and IgG1 are produced and secreted by plasma cells that are transformed by IL-4-induced B cells. When activated ILC2 cells contribute to an excess increased production of IL-4, it intensifies the type I hypersensitivity response and exacerbates allergic asthma. Our findings demonstrated that the levels of T-IgE, OVA-IgE, and OVA-IgG1 were significantly elevated in mice exposed to OVA and DBP+OVA combinations compared to saline groups ($P < 0.01$, $P < 0.01$), with a greater increase observed in the DBP+OVA group ($P < 0.01$). In particular, after the addition of the CGRP antagonist olcegepant to the experiments, the results showed that the levels of T-IgE, OVA-IgE, and OVA-IgG1 were significantly reduced in mice compared to the DBP+OVA group ($P < 0.01$). This suggests that our OVA-induced asthmatic animal model was successful and that DBP worsened the pathological changes to allergic asthma in mice through the JNC/ILC2 pathway (Fig. 7, Fig. 8).

Re-activation of JNC caused by increased IgE: According to our literature research, increased levels of IgE have been found to not only induce type I hypersensitivity responses and allergic asthma but also potentially contribute to a neuroimmune positive feedback mechanism that worsens allergic asthma. Crosson et al. [6] has shown that the high-affinity IgE receptor FcεR1 is present in the pulmonary innervated jugular venous complex ganglion (JNC) neurons and its expression is elevated in mice sensitized to specific antigens such as OVA. This suggests that the JNC immune cells may initiate neuro-immune interactions, involving lung tissue injury receptor neurons, during the development of allergic asthma if they are activated by some certain reason (such as DBP exposure). Therefore, we propose this mechanism in our scientific hypothesis. As part of our future research objectives, we aim to conduct in vitro and in vivo exposure studies on JNC neurons using different concentrations of T-IgE and OVA-IgE. These studies will help establish the qualitative and quantitative relationship between IgE and FcεR1 as well as CGRP expressed by JNC neurons. Ultimately, our findings will provide further scientific evidence to elucidate this relationship.

The innovation of this study: Exacerbation of allergic asthma by DBP is a prevalent public health issue, and its pathogenesis is relatively intricate. Although some researches including our own works have found that DBP in combination with allergen exposure increases IgE levels in allergic asthma and causes overexpression of the neuropeptide CGRP in lung tissue. However, we don't know if the elevated IgE is the cause of the abnormal expression of the neuropeptide CGRP or how CGRP activates ILC2 cells to generate neuroimmune positive feedback regulation to transmit DBP-induced adverse effects. Therefore, the highlights of our study are that (1) The "environmental adjuvant" DBP can activate neurons through the JNC pathway, causing incremental expression of the neuropeptide CGRP in lung tissues; (2) The

overexpression of CGRP can activate ILC2 and their downstream injury pathways, leading to the induction of inflammatory responses. This, in turn, promotes the activation of more injury receptor neurons, resulting in a neuroimmune positive feedback regulation of allergic asthma. This study represents the first attempt to investigate the impact of JNC/ILC2 pathway on allergic asthma from a neuroimmunology standpoint, employing molecular toxicology techniques. Additionally, we explore potential neuroimmune positive feedback mechanisms that may contribute to the progression of allergic asthma.

The shortcomings and limitations of this study: Although we initially described the neuroimmune positive feedback regulatory pathway of DBP leading to asthma exacerbation, these important associations are based on previous studies [25,57]. Zhou et al. showed that DBP aggravated asthma-like symptoms through oxidative stress and increasing CGRP, and Li et al. found that ferroptosis participated in DBP-aggravated allergic asthma in OVA-sensitized mice. And other studies suggested that CGRP is expressed by JNC cells and that this neuropeptide can activate ILC2, ILC2 play a crucial role in the development of Th2-driven allergic immune response. Through these literatures, we discovered the association between these information and realized that this would be an important neuroimmune signaling pathway, which may be involved in DBP-induced allergic asthma, so we conducted this in-depth study. Meanwhile, we also recognized that there are still several limitations to be strengthened in this study as follow: (1) Lack of the OVA + olcegepant group, it is not entirely clear whether the effect of olcegepant can be directly related to the DBP-exacerbated asthma; (2) Lack of the OVA + low dose DBP, it remains uncertain whether already lower concentration could induce adverse effects; (3) The detection of TRPV1 activation was used a single method. Subsequently, these proposed gaps will be the direction of our further research.

5. Conclusion

This study revealed that DBP can worsen OVA-induced allergic asthma. Additionally, DBP combined with OVA was found to activate JNC neurons by binding with TRPV1. This activation leads to an overexpression and release of CGRP. Notably, CGRP in lung tissue can bind to CLR expressed by and located on ILC2 immune cells, activating ILC2 cells through the transcription factor GATA3. This activation causes the synthesis and release of Th2 inflammatory cytokines, particularly IL-4. IL-4 promotes the transformation of B cells into plasma cells capable of secreting IgE, resulting in an increase in IgE concentration in lung tissue. Excessive IgE can bind and interact with the high affinity IgE receptor FcεR1 expressed by JNC, leading to the reactivation of JNC. Consequently, a vicious cycle of neural immune positive feedback is formed, exacerbating the occurrence and development of allergic asthma.

Environmental implication

The plasticizer dibutyl phthalate (DBP) easily enters the human body via inhalation and has been linked to allergic asthma. We elucidate the mechanisms of how DBP triggers allergic asthma through a novel approach of "neural-immune interactions". Here, we found that exposure to DBP activated JNC neurons, which subsequently released the neuropeptide CGRP in lung tissues of OVA mice. CGRP further activated ILC2 and promoted the release of Th2 cytokines through GATA phosphorylation, contributing to the development of airway inflammation. Increased Th2 cytokines also triggered the IgE production, which interacts with FcεR1 on JNC neurons, thereby mediating neuro-immune positive feedback regulation.

CRediT authorship contribution statement

Yang Xu: Writing – review & editing, Supervision,

Conceptualization. **Ma Ping:** Supervision, Project administration, Funding acquisition, Conceptualization. **Wu Yang:** Methodology, Data curation. **Chen Shaohui:** Methodology. **Deng Qihong:** Supervision, Conceptualization. **Li Jinquan:** Supervision, Methodology, Conceptualization. **Peng Qi:** Methodology, Investigation, Data curation. **Yao Runming:** Supervision, Conceptualization. **Li Yan:** Methodology, Investigation, Formal analysis, Data curation. **Yan Biao:** Writing – review & editing, Validation, Investigation. **Xie Xiaomin:** Writing – original draft, Methodology, Investigation, Formal analysis, Data curation.

Declaration of Competing Interest

The authors declare that they have no known competing financial interests or personal relationships that could have appeared to influence the work reported in this paper.

Data Availability

Data will be made available on request.

Acknowledgments

This work was supported by the National Natural Science Foundation of China (42177416, 52278090), the Key Special Project for Social Development Research and Development of Xianning City Science and Technology Program (2021SFYF007), Health Commission of Hubei Province Scientific Research Project (WJ2021Z006) and Scientific Research Innovative Team of Hubei University of Science and Technology (2023T08).

Appendix A. Supporting information

Supplementary data associated with this article can be found in the online version at [doi:10.1016/j.jhazmat.2023.133360](https://doi.org/10.1016/j.jhazmat.2023.133360).

References

- Ali, M.M., Sahar, T., Firyal, S., Ijaz, M., Majeed, K.A., Awan, F., et al., 2022. Assessment of cytotoxic, genotoxic, and oxidative stress of dibutyl phthalate on cultured bovine peripheral lymphocytes. *Oxid Med Cell Longev*, 9961513.
- Assas, M.B., Wakid, M.H., Zakai, H.A., Miyano, J.A., Pennock, J.L., 2016. Transient receptor potential vanilloid 1 expression and function in splenic dendritic cells: a potential role in immune homeostasis. *Immunology* 147 (3), 292–304.
- Biswas, S., Mahmud, S., Mita, M.A., Afrose, S., Hasan, M.R., Sultana Shimu, M.S., et al., 2021. Molecular docking and dynamics studies to explore effective inhibitory peptides against the spike receptor binding domain of SARS-CoV-2. *Front Mol Biosci* 8, 791642.
- Bujak, J.K., Kosmala, D., Majchrzak-Kuligowska, K., Bednarczyk, P., 2021. Functional expression of TRPV1 ion channel in the canine peripheral blood mononuclear cells. *Int J Mol Sci* 22 (6) (null).
- Cardoso, V., Chesné, J., Ribeiro, H., García-Cassani, B., Carvalho, T., Bouchery, T., et al., 2017. Neuronal regulation of type 2 innate lymphoid cells via neuromedin U. *Nature* 549 (7671), 277–281.
- Crosson, T., Wang, J.C., Doyle, B., Merrison, H., Balood, M., Parrin, A., et al., 2021. FcεR1-expressing nociceptors trigger allergic airway inflammation. *J Allergy Clin Immunol* 147 (6), 2330–2342.
- Da'as, S.I., Coombs, A.J., Balci, T.B., Grondin, C.A., Ferrando, A.A., Berman, J.N., 2012. The zebrafish reveals dependence of the mast cell lineage on Notch signaling in vivo. *Blood* 119 (15), 3585–3594.
- Denney, L., Byrne, A.J., Shea, T.J., Buckley, J.S., Pease, J.E., Herledan, G.M., et al., 2015. Pulmonary epithelial cell-derived cytokine TGF-β1 is a critical cofactor for enhanced innate lymphoid cell function. *Immunity* 43 (5), 945–958.
- Esteves de Oliveira, E., de Castro E Silva, F.M., Caçador Ayupe, M., Gomes Evangelista Ambrósio, M., Passos de Souza, V., Costa Macedo, G., et al., 2019. Obesity affects peripheral lymphoid organs immune response in murine asthma model. *Immunology* 157 (3), 268–279.
- European Chemicals Bureau (ECB), 2008. Summary Risk Assessment Report. European Commission, Joint Research Centre, Institute for Health and Consumer Protection, Toxicology and Chemical Substance (TCS), European Chemicals Bureau.
- Flores, E.N., Duggan, A., Madathany, T., Hogan, A.K., Márquez, F.G., Kumar, G., et al., 2015. A non-canonical pathway from cochlea to brain signals tissue-damaging noise. *Curr Biol* 25 (5), 606–612.
- Gast, M., Preisinger, C., Nimmerjahn, F., Huber, M., 2018. IgG-independent co-aggregation of FcεRI and FcγRIIB results in Lyn- and SHIP1-dependent tyrosine phosphorylation of FcγRIIB in murine bone marrow-derived mast cells. *Front Immunol* 9, 1937.
- Hoyler, T., Klose, C.S., Souabni, A., Turqueti-Neves, A., Pfeifer, D., Rawlins, E.L., et al., 2012. The transcription factor GATA-3 controls cell fate and maintenance of type 2 innate lymphoid cells. *Immunity* 37 (4), 634–648.
- Huang, W.C., Wu, S.J., Yeh, K.W., Liou, C.J., 2022. Gypenoside A from *Gynostemma pentaphyllum* attenuates airway inflammation and Th2 cell activities in a murine asthma model. *Int J Mol Sci* 23 (14).
- Hurbain, P., Liu, Y., Strickland, M.J., Li, D., 2022. A cross-sectional analysis of associations between environmental indices and asthma in U.S. counties from 2003 to 2012. *J Expo Sci Environ Epidemiol* 32 (2), 320–332.
- Kabata, H., Moro, K., Koyasu, S., Asano, K., 2015. Group 2 innate lymphoid cells and asthma. *Allergol Int* 64 (3), 227–234.
- Kaelberer, M.M., Caceres, A.L., Jordt, S.E., 2020. Activation of a nerve injury transcriptional signature in airway-innervating sensory neurons after lipopolysaccharide-induced lung inflammation. *Am J Physiol Lung Cell Mol Physiol* 318 (5), L953–L964.
- Källsten, L., Almamoun, R., Pierozan, P., Nylander, E., Sdougkou, K., Martin, J.W., et al., 2022. Adult exposure to di-n-butyl phthalate (DBP) induces persistent effects on testicular cell markers and testosterone biosynthesis in mice. *Int J Mol Sci* 23 (15).
- Kim, S., Keum, B., Byun, J., Kim, B., Lee, K., Yeon, J., et al., 2021. Colonic mucosal immune activation in mice with ovalbumin-induced allergic airway disease: association between allergic airway disease and irritable bowel syndrome. *Int J Mol Sci* 23 (1).
- Kim, T.H., Park, Y.M., Ryu, S.W., Kim, D.J., Park, J.H., Park, J.H., 2014. Receptor interacting protein 2 (RIP2) is dispensable for OVA-induced airway inflammation in mice. *Allergy Asthma Immunol Res* 6 (2), 163–168.
- Klose, C.S.N., Mahlaköiv, T., Moeller, J.B., Rankin, L.C., Flamar, A.L., Kabata, H., et al., 2017. The neuropeptide neuromedin U stimulates innate lymphoid cells and type 2 inflammation. *Nature* 549 (7671), 282–286.
- Koning, M.T., Trollmann, I.J.M., van Bergen, C.A.M., Alvarez Saravia, D., Navarrete, M.A., Kielbasa, S.M., et al., 2019. Peripheral IgE repertoires of healthy donors carry moderate mutation loads and do not overlap with other isotypes. *Front Immunol* 10, 1543.
- Lajoie, S., Lewkowich, I., Herman, N.S., Sproles, A., Pesce, J.T., Wynn, T.A., et al., 2014. IL-21 receptor signaling partially mediates Th2-mediated allergic airway responses. *Clin Exp Allergy* 44 (7), 976–985.
- Lei, A.H., Xiao, Q., Liu, G.Y., Shi, K., Yang, Q., Li, X., et al., 2018. ICAM-1 controls development and function of ILC2. *J Exp Med* 215 (8), 2157–2174.
- Li, Y., Yan, B., Wu, Y., Peng, Q., Wei, Y., Chen, Y., et al., 2023. Ferropapilloma participates in dibutyl phthalate-aggravated allergic asthma in ovalbumin-sensitized mice. *Ecotoxicol Environ Saf* 256, 114848.
- Lin, J.H., Yu, Y.W., Chuang, Y.C., Lee, C.H., Chen, C.C., 2021. ATF3-expressing large-diameter sensory afferents at acute stage as bio-signatures of persistent pain associated with lumbar radiculopathy. *Cells* 10 (5).
- Lu, C., Liu, Q., Deng, M., Liao, H., Yang, X., Ma, P., 2023. Interaction of high temperature and NO2 exposure on asthma risk: In vivo experimental evidence of inflammation and oxidative stress. *Sci Total Environ* 869, 161760.
- Lu, C., Wang, F., Liu, Q., Deng, M., Yang, X., Ma, P., 2023. Effect of NO2 exposure on airway inflammation and oxidative stress in asthmatic mice. *J Hazard Mater* 457, 131787.
- Lu, C., Wang, F., Qiao, Z., Deng, M., Liu, Q., Yang, X., 2023. Extreme temperatures exacerbated oxidative stress and airway inflammation in a mouse model of allergic asthma. *Allergy* 15883.
- Luo, P., Li, X., Wu, X., Dai, S., Yang, Y., Xu, H., et al., 2019. Preso regulates NMDA receptor-mediated excitotoxicity via modulating nitric oxide and calcium responses after traumatic brain injury. *Cell Death Dis* 10 (7), 496.
- Mahajan, A., Youssef, L.A., Cleyrat, C., Grattan, R., Lucero, S.R., Mattison, C.P., et al., 2017. Allergen valency, dose, and FcεRI occupancy set thresholds for secretory responses to pen a 1 and motivate design of hypoallergens. *J Immunol* 198 (3), 1034–1046.
- Mall, C., Skicisel, G.D., Proia, D.A., Mirsoian, A., Grossenbacher, S.K., Pai, C.S., et al., 2016. Repeated PD-1/PD-L1 monoclonal antibody administration induces fatal xenogeneic hypersensitivity reactions in a murine model of breast cancer. *Oncoimmunology* 5 (2), e1075114.
- Matsushita, K., Tanaka, H., Yasuda, K., Adachi, T., Fukuoka, A., Akasaki, S., et al., 2020. Regnase-1 degradation is crucial for IL-33- and IL-25-mediated ILC2 activation. *JCI Insight* 5 (4) (null).
- Mindt, B.C., Krisna, S.S., Duerr, C.U., Mancini, M., Richer, L., Vidal, S.M., et al., 2021. The NF-κB transcription factor c-rel modulates group 2 innate lymphoid cell effector functions and drives allergic airway inflammation. *Front Immunol* 12, 664218.
- Miyano, K., Shiraishi, S., Minami, K., Sudo, Y., Suzuki, M., Yokoyama, T., et al., 2019. Carboplatin enhances the activity of human transient receptor potential ankyrin 1 through the cyclic AMP-protein kinase a-kinase anchoring protein (AKAP) pathways. *Int J Mol Sci* 20 (13) (null).
- Nie, Y., Feng, F., Luo, W., Sanders, A.J., Zhang, Y., Liang, J., et al., 2022. Overexpressed transient receptor potential vanilloid 1 (TRPV1) in lung adenocarcinoma harbours a new opportunity for therapeutic targeting. *Cancer Gene Ther* 29 (10), 1405–1417.
- Shen, X., Liang, M., Chen, X., Pasha, M.A., D'Souza, S.S., Hidde, K., et al., 2019. Cutting edge: core binding factor β is required for group 2 innate lymphoid cell activation. *J Immunol* 202 (6), 1669–1673.

- [38] Shirai, Y., Nakanishi, Y., Suzuki, A., Konaka, H., Nishikawa, R., Sonehara, K., et al., 2022. Multi-trait and cross-population genome-wide association studies across autoimmune and allergic diseases identify shared and distinct genetic component. *Ann Rheum Dis*.
- [39] Silano, V., Barat Baviera, J.M., Bolognesi, C., Chesson, A., Cocconcelli, P.S., Crebelli, R., et al., 2019. Update of the risk assessment of di-butylphthalate (DBP), butyl-benzyl-phthalate (BBP), bis(2-ethylhexyl) phthalate (DEHP), di-isononylphthalate (DINP) and di-isodecylphthalate (DIDP) for use in food contact materials. *EFSA J* 17 (12), e05838.
- [40] Silver, J.S., Kearley, J., Copenhaver, A.M., Sanden, C., Mori, M., Yu, L., et al., 2016. Inflammatory triggers associated with exacerbations of COPD orchestrate plasticity of group 2 innate lymphoid cells in the lungs. *Nat Immunol* 17 (6), 626–635.
- [41] Stokes, K., LaMarche, N.M., Islam, N., Wood, A., Huang, W., August, A., 2015. Cutting edge: STAT6 signaling in eosinophils is necessary for development of allergic airway inflammation. *J Immunol* 194 (6), 2477–2481.
- [42] Strecker, T., Koulchitsky, S., Dieterle, A., Neuhuber, W.L., Weyand, M., Messlinger, K., 2008. Release of calcitonin gene-related peptide from the jugular-nodose ganglion complex in rats—a new model to examine the role of cardiac peptidergic and nitrenergic innervation. *Neuropeptides* 42 (5-6), 543–550.
- [43] Suh, D.H., Trinh, H.K., Liu, J.N., Pham, Ie D., Park, S.M., Park, H.S., et al., 2016. P2Y12 antagonist attenuates eosinophilic inflammation and airway hyperresponsiveness in a mouse model of asthma. *J Cell Mol Med* 20 (2), 333–341.
- [44] Sui, P., Wiesner, D.L., Xu, J., Zhang, Y., Lee, J., Van Dyken, S., et al., 2018. Pulmonary neuroendocrine cells amplify allergic asthma responses. *Science* 360 (6393).
- [45] Talbot, S., Abdunour, R.E., Burkett, P.R., Lee, S., Cronin, S.J., Pascal, M.A., et al., 2015. Silencing nociceptor neurons reduces allergic airway inflammation. *Neuron* 87 (2), 341–354.
- [46] Wallrapp, A., Riesenfeld, S.J., Burkett, P.R., Abdunour, R.E., Nyman, J., Dionne, D., et al., 2017. The neuropeptide NMU amplifies ILC2-driven allergic lung inflammation. *Nature* 549 (7672), 351–356.
- [47] Wang, X., Lv, Z., Han, B., Li, S., Yang, Q., Wu, P., et al., 2021. The aggravation of allergic airway inflammation with dibutyl phthalate involved in Nrf2-mediated activation of the mast cells. *Sci Total Environ* 789, 148029.
- [48] Wang, Y., Tye, A.E., Zhao, J., Ma, D., Raddant, A.C., Bu, F., et al., 2019. Induction of calcitonin gene-related peptide expression in rats by cortical spreading depression. *Cephalalgia* 39 (3), 333–341.
- [49] Wu, G., Zhang, X., Chen, X., Wang, J., Yang, J., Wang, L., et al., 2020. *Streptococcus pneumoniae* aminopeptidase N regulates dendritic cells that attenuates type-2 airway inflammation in murine allergic asthma. *Br J Pharm* 177 (22), 5063–5077.
- [50] Xun, Q., Kuang, J., Yang, Q., Wang, W., Zhu, G., 2021. GLCCI1 reduces collagen deposition and airway hyper-responsiveness in a mouse asthma model through binding with WD repeat domain 45B. *J Cell Mol Med* 25 (14), 6573–6583.
- [51] Yagi, R., Zhong, C., Northrup, D.L., Yu, F., Bouladoux, N., Spencer, S., et al., 2014. The transcription factor GATA3 is critical for the development of all IL-7R α -expressing innate lymphoid cells. *Immunity* 40 (3), 378–388.
- [52] Yan, B., Sun, Y., Zeng, J., Chen, Y., Li, C., Song, P., et al., 2019. Combined use of vitamin E and nimodipine ameliorates dibutyl phthalate-induced memory deficit and apoptosis in mice by inhibiting the ERK 1/2 pathway. *Toxicol Appl Pharm* 368, 1–17.
- [53] Ying, X., Lin, J., Yuan, S., Pan, C., Dong, W., Zhang, J., et al., 2022. Comparison of pulmonary function and inflammation in children/adolescents with new-onset asthma with different adiposity statuses. *Nutrients* 14 (14).
- [54] Zhang, L., Ying, Y., Chen, S., Arnold, P.R., Tian, F., Minze, L.J., et al., 2021. The transcription factor RelB restrains group 2 innate lymphoid cells and type 2 immune pathology in vivo. *Cell Mol Immunol* 18 (1), 230–242.
- [55] Zhao, H., Moarbes, V., Gaudreault, V., Shan, J., Aldossary, H., Cyr, L., et al., 2019. Sex differences in IL-33-induced STAT6-dependent type 2 airway inflammation. *Front Immunol* 10, 859.
- [56] Zheng, R., Chen, Y., Shi, J., Wang, K., Huang, X., Sun, Y., et al., 2020. Combinatorial IL-17rb, ST2, and TSLPR signaling in dendritic cells of patients with allergic rhinitis. *Front Cell Dev Biol* 8, 207.
- [57] Zhou, S., Han, M., Ren, Y., Yang, X., Duan, L., Zeng, Y., et al., 2020. Dibutyl phthalate aggravated asthma-like symptoms through oxidative stress and increasing calcitonin gene-related peptide release. *Ecotoxicol Environ Saf* 199, 110740.